bioRxiv preprint doi: https://doi.org/10.1101/078758; this version posted October 2, 2016. The copyright holder for this preprint (which was not certified by peer review) is the author/funder. All rights reserved. No reuse allowed without permission.

Targeted electrical stimulation of active brain sources using reciprocity

Jacek P. Dmochowski, Laurent Koessler, Lucas C. Parra, Marom Bikson, and Anthony M. Norcia

September 30, 2016

Abstract

The notion of recording neural activity and using it to guide electrical stimulation is a concept that is pervasive across ongoing efforts to modulate brain function. In particular, electroencephalography (EEG) and transcranial electrical stimulation (TES) are linked by a long-standing reciprocity principle which, despite being known for over a century, has not led to a formalism for rationally performing EEG-TES. Here we formulate the EEG and TES forward problems as a pair of linear systems with a common transfer matrix. We employ this dual formulation to derive a least-squares solution to the TES montage that generates an electric field most closely matched to the underlying activation pattern. We show that this can be performed without explicitly localizing the sources of activity. Boundary-element model (BEM) simulations using a realistic head model are then used to validate the formulation and to demonstrate that reciprocal TES guides the electric field to the location and orientation of the measured activity. These results have application to a host of clinical and research applications in which one seeks to modulate the sources of observed neural activity.

Introduction

The ability to systematically modify observed patterns of neural activity would be highly beneficial on at least two fronts: in basic neuroscience, mapping out the relationship between structure and function hinges on our ability to causally manipulate brain activity. Moreover, techniques capable of modulating brain function would provide novel strategies for combating the many psychiatric and neurological disorders marked by aberrant neural dynamics (Uhlhaas and Singer, 2006, 2012). In many cases, it would be highly desirable to either amplify or suppress an observed pattern of activity. A compelling approach to such systematic modification of brain function is to combine neuroimaging with brain stimulation (Berényi et al., 2012; Bestmann and Feredoes, 2013; Bergmann et al., 2016, 2012; Siebner et al., 2009). The technology for integrated stimulation-recording approaches to brain stimulation is in place. This is true for invasive microelectrode arrays (Maynard et al., 1997; Jimbo et al., 2003; Dostrovsky et al., 2000), deep brain stimulation (DBS) (Kent and Grill, 2013; Lempka and McIntyre, 2013; Rosin et al., 2011), depth electrodes (Rosenberg et al., 2009), cortical surface electrode arrays (Trebuchon et al., 2012), brain machine interfaces (Guggenmos et al., 2013), and non-invasive scalp electrode arrays that are commonly used in human neuroscience (Thut et al., 2005; Faria et al., 2012). However, missing is a general formalism for how to employ measurements of neural activity to design optimal stimulation parameters.

One particulalrly compelling approach is to combine, electroencephalography (EEG) with transcranial electrical stimulation (TES), mirror-symmetric processes related by the long-standing reciprocity principle introduced by Helmholtz (1853). Simply stated, the electrical path from a neural source to a (recording) electrode is equivalent to the electrical path from the (now stimulating) electrode to the location of the neural source (Rush and Driscoll, 1969). Intuition suggests that reciprocity should allow one to leverage the information carried by EEG signals to guide the parameters of the TES. However, a general principle for mapping recorded EEG potentials to stimulation parameters that target the underlying neural activity has eluded the field.

Here we develop a general formalism for combined EEG-TES. We specifically focus on the problem of how to appy the stimulation in such a way that the generated electric field is spatially matched to the neural activation pattern. By formulating both the EEG and TES signal models in a linear systems framework linked by a common transfer matrix, we derive a least-squares solution to the problem of

bioRxiv preprint doi: https://doi.org/10.1101/078758; this version posted October 2, 2016. The copyright holder for this preprint (which was not certified by peer review) is the author/funder. All rights reserved. No reuse allowed without permission.

determining a TES stimulation configuration ("montage") that generates an electric field most closely matched to the activation pattern. Importantly, we show that biological current sources in the brain may be targeted using only their projections of the scalp, and that solving the EEG inverse problem is not necessary in order to xxx. However, we further show that the problems inherent to EEG localization are shared by TES targeting, in that the two are dual problems.

In order to validate the proposed approach, we conduct boundary element model (BEM) simulations using a realistic, MRI-based human head model. We quantify the limits on the achievable electric field focality and intensity using reciprocal TES. We also show that reciprocal TES accounts for varying source orientation, in that both radial and tangential sources are xxx. We conclude by illustrating a scenario in which reciprocal TES fails. In summary, we demonstrate that causal manipulation of neural sources may be achieved by using surface recordings of their activity to design spatially patterned electrical stimulation. They pave the way for closed-loop brain stimulation technology.

Results

Reciprocal electrical stimulation

Imagine an array of electrodes that is capable of both recording electric potentials and stimulating the surrounding tissue with applied electrical currents. The recorded potentials V are a linear superposition of very many neural current sources D:

$$V = RD, \tag{1}$$

where R is the electrical path between neural current sources and recording electrodes electrodes. The stimulation currents I generate an electric field E inside the brain:

$$E = SI, \tag{2}$$

where S captures the relationship between the applied stimulation currents and resulting electric field. In this multiple electrode context, reciprocity leads to a symmetry relationship among R and S:

$$R^T = S. \tag{3}$$

where ^{T} denotes matrix transposition. A derivation of (3) is provided in the Supplementary Materials. Essentially, (3) states that the electrical path from electrode-to-source is equivalent to that from source-to-electrode. Below, this relationship is exploited to selectively target the active neural sources with appropriately tuned applied currents.

Our goal is to modulate the active sources of neural activity. This entails generating an electric field that is strong at the locations of the active sources. An ideal outcome is thus $E = cD$, where c is a proportionality scalar. The selection of applied currents to make the resulting electric field proportional to the neural activity can be formulated as a convex optimization problem:

$$\begin{aligned} I^* &= \arg\min_I \|E - cD\|^2 \\ &= c\left(RR^T\right)^{-1} V. \end{aligned} \tag{4}$$

The result of (17) states that to modulate the sources of an observed pattern V, one should apply surface currents according to $c\left(RR^T\right)^{-1} V$, which is a spatially decorrelated version of V. This is in contrast to the intuitive and often used approach $I^* = V$. Its key implication is that in order to modulate neural activity patterns, one need not know the locations of the active sources but only their projection to the array. The result (17) corresponds to "excitatory" stimulation: that is, when we are looking to augment the sources of the activity observed on the array. If one seeks to inhibit the activity of the underlying sources, the applied currents take the form $I^* = -c\left(RR^T\right)^{-1} V$.

The duality of source localization and targeting. The electric field achieved by applying I^* is equivalent to the minimum-norm least-squares estimate of D given V.

$$R^T I^* = \arg\min_D \|D\|_2 \text{ subject to } V = RD \tag{5}$$

$$= D^* \tag{6}$$

This relation states that the electric field achieved by the set of reciprocating currents I^* is proportional to the minimum-norm source estimate of the neural activity D. This implies that targeting in brain

bioRxiv preprint doi: https://doi.org/10.1101/078758; this version posted October 2, 2016. The copyright holder for this preprint (which was not certified by peer review) is the author/funder. All rights reserved. No reuse allowed without permission.

stimulation is a dual problem to source localization in brain imaging, and that the inherent limitations in these processes are common to both.

The approach presented here pertains to the case of an array of N surface electrodes (for example, electrocorticography (ECoG) grids or scalp EEG arrays) where each electrode is capable of both recording neural activity and electrically stimulating the surrounding tissue.

Simulation Results

To confirm the analytical results and to estimate the performance of reciprocal brain stimulation in humans, we conducted a boundary-element model (BEM) simulation employing a magnetic resonance imaging (MRI)-based head model (see Methods for details). Activation of dipolar current sources spanning an average radius of 1.03 cm were simulated and the resulting scalp potentials were fed into both the "naive" and true reciprocity formulations (Fig. 1A shows an example activation in primary motor cortex). To quantify stimulation performance, we computed the ratio of the electric field strength at the activation region to the strength outside the activation. Naive reciprocity produced a diffuse electric field, with an electric field ratio of 1.76 ± 0.61 (Fig. 1C-D; $N = 15002$, mean $\pm$ standard deviation). A more focused electric field was achieved by reciprocal stimulation, with the field inside the activation region being 10.67 ± 8.68 stronger than the field outside of it (Fig. 1E-F; $p < 0.001$, paired, right-tailed Wilcoxon signed rank test). The increased focality of the electric field comes at the expense of reduced field strength at the activation site: naive reciprocity achieves an electric field of 0.20 ± 0.087 V/m at the activation, compared to 0.086 ± 0.054 V/m for reciprocal stimulation. As predicted by Theorem 3, the electric field achieved by reciprocal stimulation is collinear with the minimum-norm source estimate of the simulated EEG pattern (Pearson correlation coefficient = 1 for all activations; compare source estimate in Fig. 1B with achieved electric field in E).

To compare the tDCS montages extracted by reciprocity across a variety of brain regions, we simulated bilateral activation of four regions-of-interest (ROIs) from the Destrieux cortical surface parcellation atlas (REFS) (Figure 3A). Activation of each ROI resulted in dipolar scalp topographies (Figure 3B) spanning broad regions of the scalp. Such topographies are often observed in sensory and cognitive EEG research (REFS). The tDCS montages that reciprocated these topographies exhibited substantial variation across ROIs (Fig 3C). In particular, the montages consistes of both anodes and cathodes in the scalp locations that exhibited positive scalp activation. Note, for example, that the tDCS montage that reciprocates activation of the superior parietal lobule consists of two strong cathodes and two strong anodes in a "T" configuration. In other words, positive (negative) scalp potentials do not map neatly onto anodal (cathodal) stimulation. For the ROI activations simulated here, the frontal and parietal montages generated the largest electric field intensities, while the electric field strength over the temporal and occipital targets were more modest. xxx These results demonstrate the reciprocating EEG topographies is a non-trivial procedure that would be difficult to approximate using manual techniques.

Due to the folded structure of cortex, the pyramidal neurons that are thought to give rise to the EEG (REFS) are oriented either radially or tangentially to the scalp surface, depending on whether they lie on a gyrus or sulcus, respectively. We sought to determine whether reciprocal tDCS is able to produce electric fields that "handle" these two orientations: that is, whether the resulting electric fields are focused at the activated tissue and with the desired orientation (normal to the cortical surface). We therefore simulated one gyral and one sulcal activation in the left motor cortex of the ICBM-152 head model, with the activations separated by a distance of x mm (left panels of Figs 4 A,D). Gyral activation led to a focal, monopolar pattern over the left central scalp electrodes (right panel of Fig 4 A). The reciprocal tDCS montage for this scalp topography was marked by a dominant central anode with surrounding cathodes in a "ring" configuration (Figure 4 B). The electric field produced by this montage approached a magnitude of 0.25 V/m in the direction perpendicular to the cortical sheet, while the nearby sulcal tissue was only slightly polarized (X V/m; Figure 4 C). Activation of the sulcal tissue resulted in an antisymmetric dipolar pattern over fronto-central electrodes (right panel of Figure 4 D). The tDCS montage that reciprocated this activation differed from the radial one, as a strong cathode appeared at a left anterior location (Figure 4 E). While the resulting electric field was selective to the sulcal tissue (ratio of sulcal to gyral electric field was Y mm), the magnitude of the electric field at the targeted tissue was much lower than that when targeting a gyrus (< 0.05 V/m, Figure 4 F).

bioRxiv preprint doi: https://doi.org/10.1101/078758; this version posted October 2, 2016. The copyright holder for this preprint (which was not certified by peer review) is the author/funder. All rights reserved. No reuse allowed without permission.

Discussion

Reciprocity does not solve the inverse problem of EEG. Here we have shown how measured EEG potentials may be translated into TES montages that produce electric fields focussed over the areas of the neural activation. The solution to the EEG-TES reciprocity problem is to spatially decorrelate the vector of scalp potentials by the matrix a. By spatially decorrelating the observed scalp potentials, a TES montage producing an electric field that best approximated the underlying neural activation was generated. Notably, the determination of the reciprocal TES montage did not require source localization of the EEG: the square matrix being inverted in (X) has as many columns as the number of scalp electrodes and is therefore readily invertible. However, this does *not* imply that reciprocity has solved the ill-posed inverse problem of EEG. Rather, it was shown that source localization of EEG and targeting of TES are actually dual sides of the same mathematical problem. Thus, if trying to reciprocate an EEG topography that would fail to yield a meaningful source estimate via minimum-norm, the resulting TES targeting would also fail to stimulate the source of the activity. Nevertheless, the presented approach allows for the targeting of brain regions having observed only their projections to the scalp.

Constraining for safety. The unconstrained reciprocity equation generally yields current distributions that are large and thus unsafe. Therefore, a downscaling of the reciprocal montage is required in practice. Here this downscaling was to maintain the "direction" of the applied current vector while restricting its magnitude to a safe value. This means that the restricted montage produces a field that is linearly dependent (proportional) to that produced by the unconstrained montage. Another option may have been to search the current space to find a montage that yields the most reciprocal montage within the safe region. The fact that the desired electric field distribution is not available prevents the application of conventional l-1 constrained least squares techniques to this problem.

Limits on focality. Given the limits imposed by the number of electrodes (i.e., 64) and the maximum current delivered (i.e., 2 mA), the maximum focality to the dorsal surface of the cortex was here found to be approximately 3 cm. This represents.... The maximum intensity was found to be 0.3 V/m, with these maxima values found as "hotspots" along patches of the cortical surface. For both focality and intensity, targeting sources located along the ventral surface was found to be challenging, with simultaneously low focality and intensity produced by reciprocal TES to those regions. Both focality and intensity may be improved by the inclusion of low-lying electrodes (for example, on the neck) that provide coverage of ventral surfaces.

Practical implementation. The EEG is generally a time-varying multichannel vector that is commonly represented as a space-time data matrix. Reciprocal TES takes as an input a vector of scalp potentials, meaning that this data matrix must be converted into a column vector. This can be accomplished in a few ways. The simplest way would be to take a simple temporal average of the data and reciprocate the time-averaged EEG activation. Another possibility is to decompose the data into spatial components via a technique such as PCA, ICA, or RCA. One could then select one component to be the input to the reciprocity scheme.

Consolidating efforts. There are presently a number of software packages that generate forward models (also known as "lead field" matrices) for EEG (REFS). These are almost always surface-based BEM where the source space is along the cortical surface where the presumed sources of the EEG lie (REFS). Reciprocity (see Equation Y) means that these forward models are equally valid for modeling TES. Conversely, much effort has been invested into the generation of finite element models (FEM) of the current flow induced by TES. Here the source space is volumetric as we are interested in ... These models are similarly applicable to the ... The only caveat is that a conversion of units must be performed in order to appropriately convert between units of dipole moments to the electric field (see Methods eqn Z). Note that TES of deep sources is equivalent to the strong expression of deep dipoles via volume conduction.

Towards closed-loop stimulation. Closed loop stimulation has been found to be effective across a variety of domains. The technique proposed here allows one to switch between recording and stimulation in a purely non-invasive manner using only surface measurements. This can be extended to other applications such as microelectrode arrays, for example.

Methods

On the recording side, each electrode captures a mixture of electrical activity generated by M biological current sources which are modeled here as electric dipoles. The biophysics of volume conduction dictate that the "channel" between each such biological source and each surface electrode is linear, meaning that

bioRxiv preprint doi: https://doi.org/10.1101/078758; this version posted October 2, 2016. The copyright holder for this preprint (which was not certified by peer review) is the author/funder. All rights reserved. No reuse allowed without permission.

we can formulate the problem in matrix form as:

$$\begin{aligned} V &= RD \\ &= \begin{bmatrix} R^{(x)} & R^{(y)} & R^{(z)} \end{bmatrix} \begin{bmatrix} D^{(x)} \\ D^{(y)} \\ D^{(z)} \end{bmatrix}, \end{aligned} \tag{7}$$

where V denotes the N-element vector of surface electric potentials (units of Volts), R is the N-by-$3M$ mixing matrix relating neural activations in the brain to electric potentials on the surface (units of Ωm^{-1}), $R^{(i)}$ is a submatrix of R capturing the i-component of the mixing matrix where the index i spans the three Cartesian dimensions $i \in \{x, y, z\}$, D is the $3M$-element source vector modeling the intensity of each dipole (units of $A \cdot m$), and $D^{(i)}$ is a subvector of D which captures the i-component of the dipole field. The element at row n, column m of $R^{(i)}$ corresponds to the electric potential generated between electrode n and a designated reference electrode when dipole m is activated with unit strength (i.e, 1 $A \cdot m$) in direction i.

Turning now to the stimulation side, we model the electric field generated inside the brain as a linear function of the applied electric currents across the array:

$$\begin{aligned} E &= \begin{bmatrix} E^{(x)} \\ E^{(y)} \\ E^{(z)} \end{bmatrix} \\ &= \begin{bmatrix} S^{(x)} \\ S^{(y)} \\ S^{(z)} \end{bmatrix} I \\ &= SI, \end{aligned} \tag{8}$$

where the $3N$-element vector E represents the external electric field generated inside the brain during stimulation, $E^{(i)}$ is a subvector of E capturing the i-component of the generated electric field, S is a $3N$-by-M lead-field matrix which relates applied currents across the array to induced electric fields inside the brain, $S^{(i)}$ is a submatrix of S capturing the i-component of the lead field matrix, and I is an N-element vector modeling the applied currents across the surface array. The element at row m, column n of $S^{(i)}$ corresponds to the i-component of the electric field achieved at source location n by applying a unit current to surface electrode n and a current of -1 A to the designated reference electrode.

Note that we have assumed that a reference electrode is common to both the recording and stimulation arrangements. During stimulation, the current applied to the reference is equal to the negative of the sum across elements of I.

Theorem 1. *Reciprocity in linear algebraic terms.*

$$R^{(i)^T} = S^{(i)^T}, \quad i \in \{x, y, z\}. \tag{9}$$

where ^{T} denotes matrix transposition. This is the reciprocity equation stated in linear algebraic terms. Due to its cumbersome nature, I defer the derivation to the appendix. This relation states that the path from scalp-to-brain is symmetric as that from brain-to-scalp. While this relation is seemingly obvious, it has apparently not been stated, and importantly, the numerical computations of matrices R and S have been carried out separately in the field of EEG and TES modeling.

Proof. (Theorem 1)

The fundamental reciprocity relation, when written for the case of a single dipole in the brain and a single electrode pair on the scalp is given by (Rush and Driscoll, 1969):

$$\begin{aligned} V_{n_o} &= \frac{E_{m_o}^T D_{m_o}}{I_{n_o}} \\ &= \frac{E_{m_o}^{(x)} D_{m_o}^{(x)} + E_{m_o}^{(y)} D_{m_o}^{(y)} + E_{m_o}^{(z)} D_{m_o}^{(z)}}{I_{n_o}}, \end{aligned} \tag{10}$$

where V_{n_o} is the voltage at scalp location n_o (relative to a reference electrode) due to an activation D_{m_o} at brain location m_o, and reciprocally, E_{m_o} is the electric field generated at brain location m_o when applying a current of I_{n_o} to scalp location n_o (and hence a current of -I_{n_o} at the reference electrode).

bioRxiv preprint doi: https://doi.org/10.1101/078758; this version posted October 2, 2016. The copyright holder for this preprint (which was not certified by peer review) is the author/funder. All rights reserved. No reuse allowed without permission.

Moreover, we have explicitly written out the x-, y-, and z- components of the electric field as $E_{m_o}^{(x)}$, $E_{m_o}^{(y)}$, and $E_{m_o}^{(z)}$, respectively, with analogous definitions holding for the electric dipole D_{m_o}.

We seek to extend this result to the case of multiple dipolar sources in the brain (indexed by m) and multiple electrode pairs on the scalp (indexed by n). Invoking the superposition principle on (10) yields:

$$V_n = \sum_m \frac{E_{nm}^{(x)} D_m^{(x)} + E_{nm}^{(y)} D_m^{(y)} + E_{nm}^{(z)} D_m^{(z)}}{I_n}, \tag{11}$$

where $E_{nm}^{(i)}$ is i-component of the electric field generated at brain location m when stimulating at scalp electrode n, $i \in \{x, y, z\}$. We can express (11) in matrix notation as:

$$\begin{aligned} V &= RD \\ &= \begin{bmatrix} R^{(x)} & R^{(y)} & R^{(z)} \end{bmatrix} \begin{bmatrix} D^{(x)} \\ D^{(y)} \\ D^{(z)} \end{bmatrix}, \end{aligned} \tag{12}$$

where

$$R_{nm}^{(i)} = E_{nm}^{(i)} / I_n \tag{13}$$

is the element at row n and column m of N-by-M matrix $R_{nm}^{(i)}$.

Let us turn now to the stimulation case. We seek to write the net electric field generated in the brain when simultaneously stimulating at multiple surface electrodes (indexed by n). Once again employing the superposition principle, we write the total electric field as the sum of the individual electric fields generated by stimulation at each surface electrode:

$$E_m^{(i)} = \sum_n E_{nm}^{(i)}, \tag{14}$$

where $E_m^{(i)}$ is the i-component of the net electric field at brain location m. From (13), we have that $E_{nm}^{(i)} = R_{nm}^{(i)} I_n$, which we substitute into (14) to yield:

$$E_m^{(i)} = \sum_n R_{mn}^{(i)} I_n. \tag{15}$$

Writing (15) in matrix notation leads to:

$$\begin{pmatrix} E_1^{(i)} \\ E_2^{(i)} \\ \vdots \\ E_M^{(i)} \end{pmatrix} = \begin{pmatrix} R_{11}^{(i)} & R_{12}^{(i)} & \dots & R_{1N}^{(i)} \\ R_{21}^{(i)} & R_{22}^{(i)} & \dots & R_{2N}^{(i)} \\ \vdots & \vdots & \ddots & \vdots \\ R_{M1}^{(i)} & R_{M2}^{(i)} & \dots & R_{MN}^{(i)} \end{pmatrix} \begin{pmatrix} I_1 \\ I_2 \\ \vdots \\ I_N \end{pmatrix}, \tag{16}$$

from which we identify $S_{mn}^{(i)} = R_{nm}^{(i)}$, or $R^{(i)} = {S^{(i)}}^T$, which is the desired result. □

Imagine now that one observes a patten of activity on the array, and seeks to modulate the brain sources that generated this activity. This may correspond to the case of a neural correlate of pathological activity such as a spike-and-wave complex in epilepsy, or activity evoked by an experimental paradigm that one is investigating. Our goal is to drive the stimulation current into the locations of the neural sources. Mathematically, this involves selecting the applied currents I such that the resulting electric field E is proportional to D: brain sources with a strong activation receive a lot of external stimulation, while inactive sources are spared. For mathematical rigor, we introduce a proportionality scalar k which maps the units of the electric field E to those of the dipole field D. The value of $k = \sigma d^3$ corresponds to the strength of a dipole source which generates an electric field of 1 V/m in a tissue of conductivity σ across a distance of d. In the simulations presented here, $\sigma = 0.2$ and $d = 1$ mm, leading to $k = 2 \times 10^{-10}$.

We seek to minimize the squared error betweek kE and D, leading to the following optimization problem:

$$I^* = \arg\min_I \|kE - D\|^2. \tag{17}$$

bioRxiv preprint doi: https://doi.org/10.1101/078758; this version posted October 2, 2016. The copyright holder for this preprint (which was not certified by peer review) is the author/funder. All rights reserved. No reuse allowed without permission.

Theorem 2. *Reciprocal targeting. In a least-squares sense, the vector of scalp currents I^* which reciprocates the biological field D is given by:*

$$I^* = \left(kRR^T\right)^{-1} V. \tag{18}$$

Proof. Let $J = \|kE - D\|^2$ denote the cost function to be minimized. Taking the derivative with respect to the vector of applied currents I leads to:

$$\begin{aligned}
\frac{\delta J}{\delta I} &= \frac{\delta}{\delta I} \|kE - D\|^2 \\
&= \frac{\delta}{\delta I} \; k^2 E^T E - 2kE^T D + D^T D \\
&= \frac{\delta}{\delta I} \; k^2 (R^T I)^T (R^T I) - 2k(R^T I)^T D + D^T D \\
&= \frac{\delta}{\delta I} \; k^2 I^T R R^T I - 2kI^T (RD) + D^T D \\
&= \frac{\delta}{\delta I} \; k^2 I^T R R^T I - 2kI^T V + D^T D \\
&= 2k^2 R R^T I - 2kV.
\end{aligned} \tag{19}$$

Setting (19) to zero leads to

$$kRR^T I = V,$$

from which we arrive at the desired result (20). □

This is the main result of the paper. Its key implication is that in order to target a biological field D, one need not know D but only its projection to the scalp V. The result (20) corresponds to "excitatory" stimulation: that is, when we are looking to augment the sources of the activity observed on the array. If one seeks to inhibit the activity of the underlying sources, the applied currents take the form $I^* = -\left(kRR^T\right)^{-1} V$. Finally, note that RR^T is an N-by-N matrix which is the sum of $M \gg N$ outer products; consequently, it generally has a well-defined inverse.

Theorem 3. *The duality of source localization and targeting. The electric field achieved by applying I^* is equivalent to the minimum-norm least-squares estimate of D given V.*

$$\begin{aligned}
R^T I^* &= R^T (RR^T)^{-1} V \\
&= (R^T R)^{-1} R^T V \\
&= R^{\#} V
\end{aligned} \tag{20}$$

bioRxiv preprint doi: https://doi.org/10.1101/078758; this version posted October 2, 2016. The copyright holder for this preprint (which was not certified by peer review) is the author/funder. All rights reserved. No reuse allowed without permission.

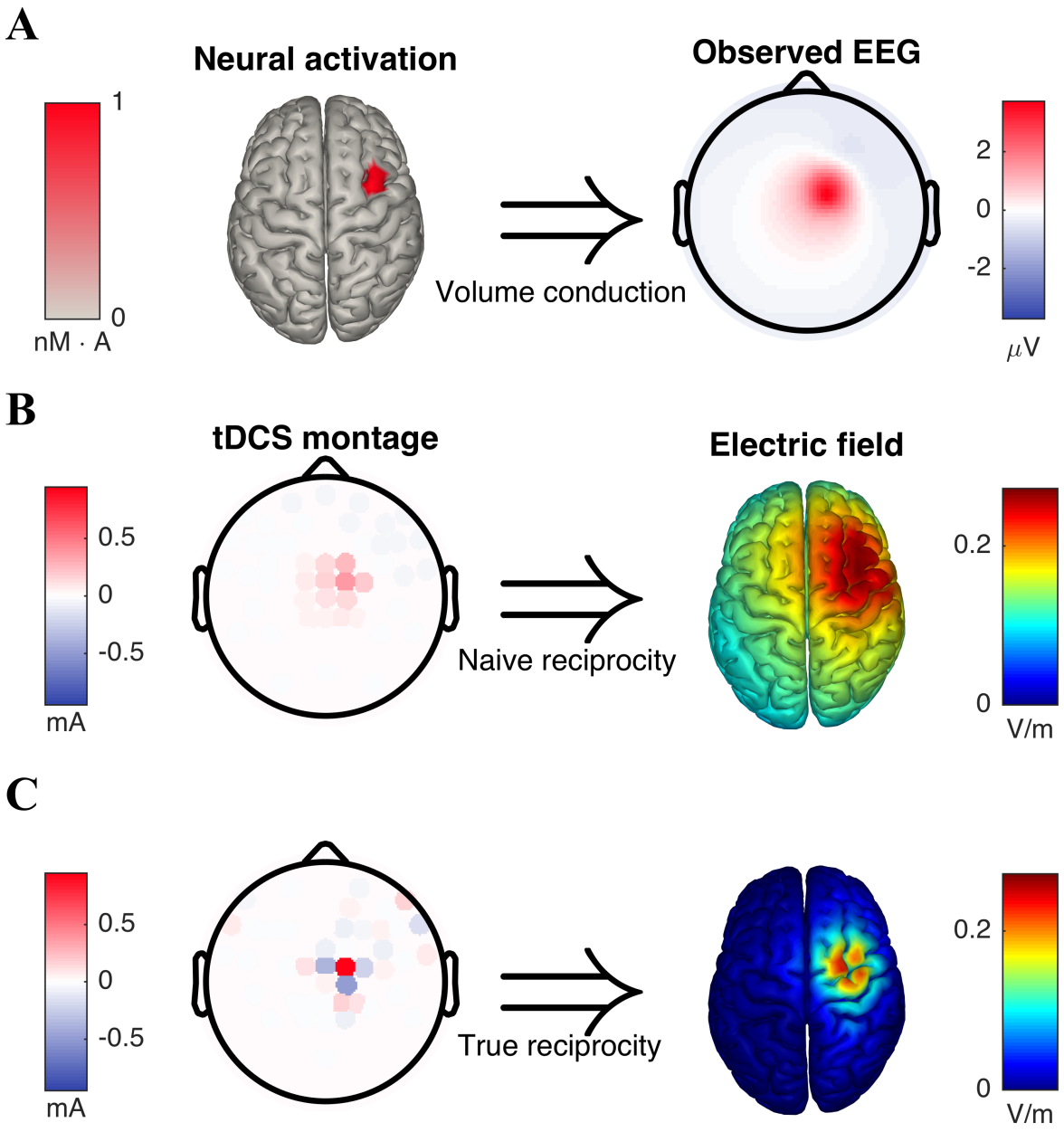

Figure 1: Reciprocal stimulation produces an electric field focused on the site of neural activation. **(A)** Activation of a dipolar source in motor cortex produces a stereotyped pattern of electric potentials on the scalp. **(B)** Source localization identifies a patch of motor cortex as the origin of the observed scalp activity. **(C)** By patterning the stimulation currents according to the observed scalp activity (i.e., set the stimulation current to the value of electric potential at each electrode), "naive" reciprocity produces a diffuse electric field in the brain. **(D** The electric field at the neural activation site is approximately twice as strong as the field outside of the activation. **(E)** Application of true reciprocity dictates that the pattern of stimulation currents required to modulate the neural source is nuanced, with both positive and negative currents injected over the source. The resulting electric field is concentrated at the location of the activated dipolar source, and is collinear with the source estimate in (B). **(F)** The achieved electric field is more then ten times stronger inside the region of activation compared to outside of it.

bioRxiv preprint doi: https://doi.org/10.1101/078758; this version posted October 2, 2016. The copyright holder for this preprint (which was not certified by peer review) is the author/funder. All rights reserved. No reuse allowed without permission.

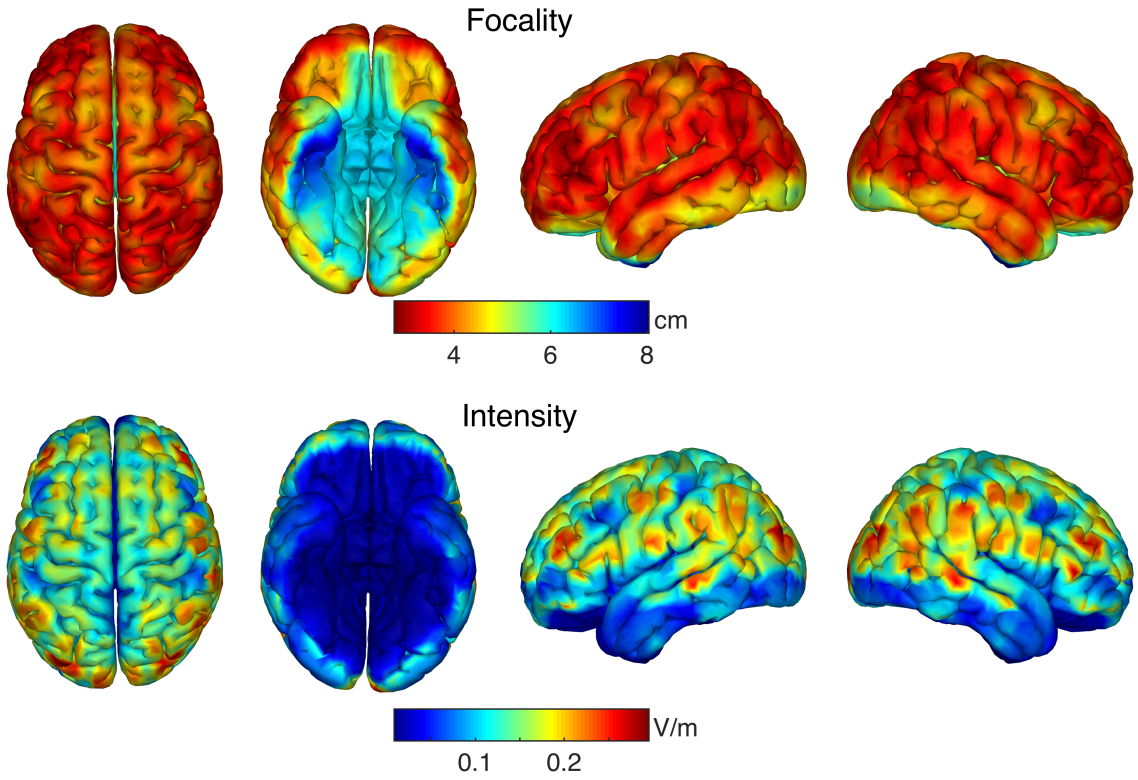

Figure 2: Ability to target brain sources varies with location. Symmetric. Ventral is hard. Focality is proportional to intensity. $r = -0.77$, $p = 0$, $N = 15002$

bioRxiv preprint doi: https://doi.org/10.1101/078758; this version posted October 2, 2016. The copyright holder for this preprint (which was not certified by peer review) is the author/funder. All rights reserved. No reuse allowed without permission.

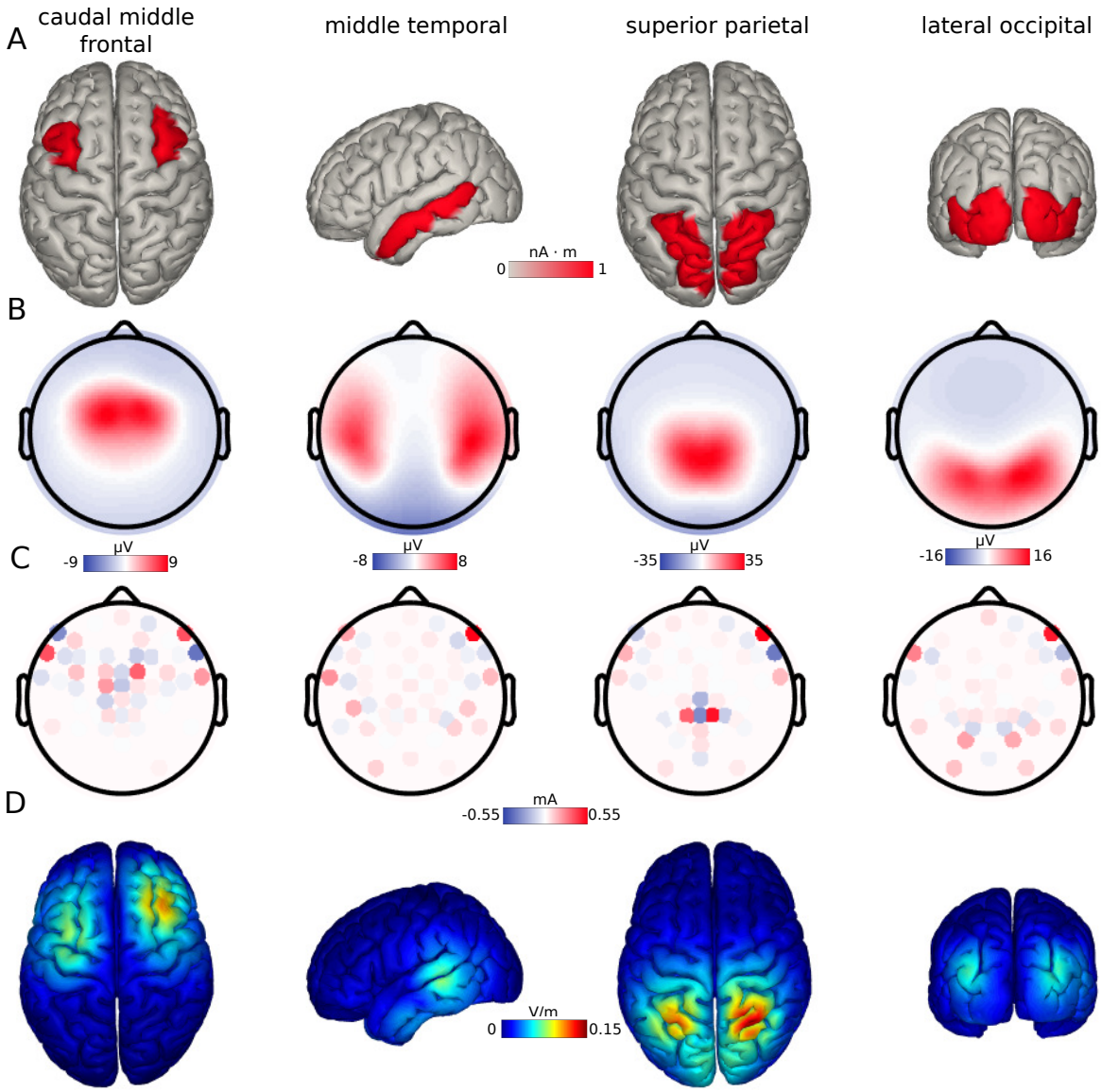

Figure 3: Reciprocal montages for a sample of anatomical regions.

bioRxiv preprint doi: https://doi.org/10.1101/078758; this version posted October 2, 2016. The copyright holder for this preprint (which was not certified by peer review) is the author/funder. All rights reserved. No reuse allowed without permission.

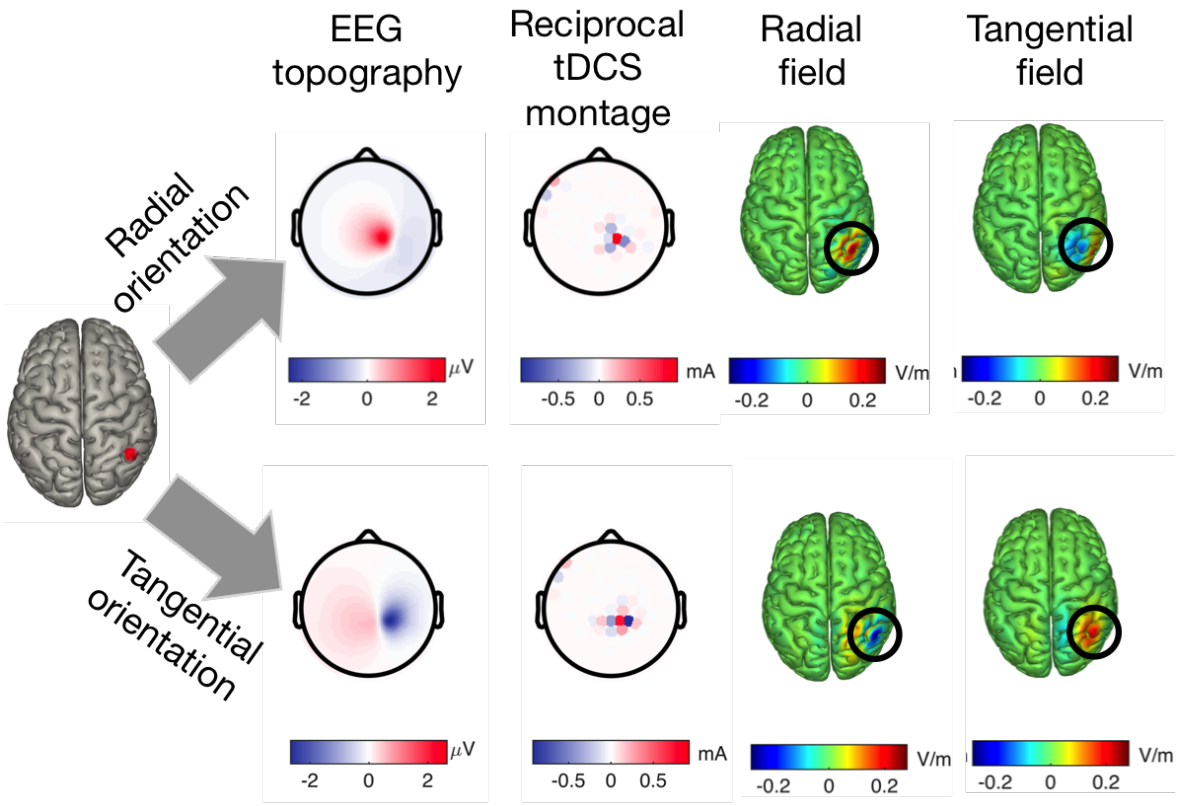

Figure 4: Reciprocal stimulationaccounts for varying source orientation.

bioRxiv preprint doi: https://doi.org/10.1101/078758; this version posted October 2, 2016. The copyright holder for this preprint (which was not certified by peer review) is the author/funder. All rights reserved. No reuse allowed without permission.

References

Berényi, A., Belluscio, M., Mao, D., and Buzsáki, G. (2012). Closed-loop control of epilepsy by transcranial electrical stimulation. *Science*, 337(6095):735–737.

Bergmann, T. O., Karabanov, A., Hartwigsen, G., Thielscher, A., and Siebner, H. R. (2016). Combining non-invasive transcranial brain stimulation with neuroimaging and electrophysiology: Current approaches and future perspectives. *NeuroImage*.

Bergmann, T. O., Mölle, M., Schmidt, M. A., Lindner, C., Marshall, L., Born, J., and Siebner, H. R. (2012). Eeg-guided transcranial magnetic stimulation reveals rapid shifts in motor cortical excitability during the human sleep slow oscillation. *The Journal of Neuroscience*, 32(1):243–253.

Bestmann, S. and Feredoes, E. (2013). Combined neurostimulation and neuroimaging in cognitive neuroscience: past, present, and future. *Annals of the New York Academy of Sciences*, 1296(1):11–30.

Dostrovsky, J., Levy, R., Wu, J., Hutchison, W., Tasker, R., and Lozano, A. (2000). Microstimulation-induced inhibition of neuronal firing in human globus pallidus. *Journal of neurophysiology*, 84(1):570–574.

Faria, P., Fregni, F., Sebastião, F., Dias, A. I., and Leal, A. (2012). Feasibility of focal transcranial dc polarization with simultaneous eeg recording: preliminary assessment in healthy subjects and human epilepsy. *Epilepsy & Behavior*, 25(3):417–425.

Guggenmos, D. J., Azin, M., Barbay, S., Mahnken, J. D., Dunham, C., Mohseni, P., and Nudo, R. J. (2013). Restoration of function after brain damage using a neural prosthesis. *Proceedings of the National Academy of Sciences*, 110(52):21177–21182.

Helmholtz, H. v. (1853). Ueber einige gesetze der vertheilung elektrischer ströme in körperlichen leitern, mit anwendung auf die thierisch-elektrischen versuche (schluss.). *Annalen der Physik*, 165(7):353–377.

Jimbo, Y., Kasai, N., Torimitsu, K., Tateno, T., and Robinson, H. P. (2003). A system for mea-based multisite stimulation. *Biomedical Engineering, IEEE Transactions on*, 50(2):241–248.

Kent, A. R. and Grill, W. M. (2013). Neural origin of evoked potentials during thalamic deep brain stimulation. *Journal of neurophysiology*, 110(4):826–843.

Lempka, S. F. and McIntyre, C. C. (2013). Theoretical analysis of the local field potential in deep brain stimulation applications. *PloS one*, 8(3):e59839.

Maynard, E. M., Nordhausen, C. T., and Normann, R. A. (1997). The utah intracortical electrode array: a recording structure for potential brain-computer interfaces. *Electroencephalography and clinical neurophysiology*, 102(3):228–239.

Rosenberg, D., Mauguiere, F., Catenoix, H., Faillenot, I., and Magnin, M. (2009). Reciprocal thalamocortical connectivity of the medial pulvinar: a depth stimulation and evoked potential study in human brain. *Cerebral Cortex*, 19(6):1462–1473.

Rosin, B., Slovik, M., Mitelman, R., Rivlin-Etzion, M., Haber, S. N., Israel, Z., Vaadia, E., and Bergman, H. (2011). Closed-loop deep brain stimulation is superior in ameliorating parkinsonism. *Neuron*, 72(2):370–384.

Rush, S. and Driscoll, D. A. (1969). Eeg electrode sensitivity-an application of reciprocity. *Biomedical Engineering, IEEE Transactions on*, (1):15–22.

Siebner, H. R., Bergmann, T. O., Bestmann, S., Massimini, M., Johansen-Berg, H., Mochizuki, H., Bohning, D. E., Boorman, E. D., Groppa, S., Miniussi, C., et al. (2009). Consensus paper: combining transcranial stimulation with neuroimaging. *Brain stimulation*, 2(2):58–80.

Thut, G., Ives, J. R., Kampmann, F., Pastor, M. A., and Pascual-Leone, A. (2005). A new device and protocol for combining tms and online recordings of eeg and evoked potentials. *Journal of neuroscience methods*, 141(2):207–217.

bioRxiv preprint doi: https://doi.org/10.1101/078758; this version posted October 2, 2016. The copyright holder for this preprint (which was not certified by peer review) is the author/funder. All rights reserved. No reuse allowed without permission.

Trebuchon, A., Guye, M., Tcherniack, V., Tramoni, E., Bruder, N., and Metellus, P. (2012). [interest of eeg recording during direct electrical stimulation for brain mapping function in surgery]. In *Annales francaises d'anesthesie et de reanimation*, volume 31, pages e87–90.

Uhlhaas, P. J. and Singer, W. (2006). Neural synchrony in brain disorders: relevance for cognitive dysfunctions and pathophysiology. *Neuron*, 52(1):155–168.

Uhlhaas, P. J. and Singer, W. (2012). Neuronal dynamics and neuropsychiatric disorders: toward a translational paradigm for dysfunctional large-scale networks. *Neuron*, 75(6):963–980.